



On the Signature of Highest Energy Particles in Gamma-Ray Bursts

Denis Gialis

► **To cite this version:**

Denis Gialis. On the Signature of Highest Energy Particles in Gamma-Ray Bursts. 2008. <hal-01297129>

HAL Id: hal-01297129

<https://hal.archives-ouvertes.fr/hal-01297129>

Submitted on 2 Apr 2016

HAL is a multi-disciplinary open access archive for the deposit and dissemination of scientific research documents, whether they are published or not. The documents may come from teaching and research institutions in France or abroad, or from public or private research centers.

L'archive ouverte pluridisciplinaire **HAL**, est destinée au dépôt et à la diffusion de documents scientifiques de niveau recherche, publiés ou non, émanant des établissements d'enseignement et de recherche français ou étrangers, des laboratoires publics ou privés.

On the Signature of Highest Energy Particles in Gamma-Ray Bursts

D. Gialis

Ph. D., Université J. Fourier, Grenoble - FRANCE

ABSTRACT

The launch of *Fermi* observatory opens new possibilities to develop diagnosis of Gamma-Ray Burst parameters, especially during their prompt emission. In this paper, first, we focus on the issue of the observability of the electron distribution cut-off, which is very sensitive to magnetic field parameters (intensity, turbulence level...). Its observability mainly depends on the importance of the Self-Synchro-Compton emission and, of γ - γ absorption process, that we calculate by taking account of the important stratification of the medium. Actually we found wide possibilities to observe or deduce the electron distribution cut-off and thus constrain magnetic parameters in the outflow of the burst. Then, we also focus on the possible gamma signature of the cosmic ray production during the prompt emission, through their synchrotron emission around a few GeV. Again we look at the γ - γ absorption process and found nevertheless favorable conditions (particularly if $B \propto 1/r$) to observe this signature for some range of magnetic parameters, when the Compton parameter is sufficiently small ($Y < 10^{-2}$).

Key words. gamma rays: bursts - radiation mechanisms: non-thermal - magnetic fields

1. Introduction

The interpretation of the Gamma-Ray Burst (hereafter GRB) prompt emission is one of the most important challenge for the “standard” internal shock model (see e.g. Piran (2005)). Also, a key ingredient, on the way of understanding, is the magnetic field; its intensity, its turbulence level and its temporal evolution in the outflow are crucial for both the particle acceleration processes and the resulting synchrotron and Self-Synchro-Compton (hereafter SSC) high energy emissions. We think that future *Fermi* observations of GRBs will provide us with some very interesting elements of diagnosis, that we want to emphasize here. In our investigation, and according to previous work (Gialis & Pelletier (2005)), we first intend to clarify and to develop some constraints on the particle acceleration efficiency in the internal shocks, following the characteristics of the magnetic field. In Sec. 2, we determine the local cut-off energy for both the accelerated particle energy distribution and their synchrotron emission and we show that the possible observation of a global energy cut-off, in the electronic synchrotron spectrum, would give us some indications on the magnetic field. In another hand, we have to take into account opacity effects, which could occur in GRB outflows and, which could prevent any observational signature relating to distribution cut-off. In Sec. 3, we then discuss about the γ - γ absorption between the highest energy photons produced by the electronic population, and the lower energy ones, and we look at which conditions it could play an important role, especially in hiding the electron distribution cut-off. In last section, we focus on the acceleration of hadronic particles, like protons: because the usual Fermi acceleration process, at internal and external shocks, seems to be inefficient to reach the UHECR energy range (see e.g. Lemoine et al. (2006), and Gialis & Pelletier (2003)), we first examine some properties of a secondary acceleration process by scattering off relativistic hydro-magnetic fronts, as previously proposed (Gialis & Pelletier (2004)). In this context, we conclude about the possibility to observe a synchrotron signature for UHECRs, depending on the magnetic parameters, against the γ - γ absorption and for a sufficiently small Compton parameter ($Y < 10^{-2}$) corresponding to a magnetic dominated outflow.

2. Evolution of the electronic distribution cut-off during the prompt emission

2.1. Theoretical framework and magnetic parameters

The internal shock model was first introduced (see e.g. Rees & Mészáros (1994)) to describe the evolution of an unsteady ultra-relativistic outflow produced by an inner engine (black hole surrounded by a magnetized torus) during a time Δt_w . The simplest version of this model assumes that the collimated outflow is constituted by a set of layers ejected at different times, with different Lorentz factors of the order of 10^2 to 10^3 , in order to solve the well-known “compactness problem”. The average Lorentz factor $\bar{\Gamma}$ can reach the value of the baryonic loading parameter $\eta = E/M_b c^2$, where E is the total energy of the burst and M_b the baryonic mass carried into the outflow.

Internal shocks occur when slower layers catch up with faster ones. These shocks are mildly relativistic, with a relative Lorentz factor in the co-moving frame $\lesssim 2$. For a typical size $r_0 = 10^7$ cm of the inner engine, and an average Lorentz factor $\bar{\Gamma}$ in the observer frame, shocks occur at a distance $r_b \simeq \bar{\Gamma}^2 r_0$ or $\eta^2 r_0$, η being the baryonic parameter ($E/M_b c^2$). In this internal shock phase, the width, ΔR , of the layers is proportional to the distance r from the black hole. Assuming that the layers are optically thin to $e^- \gamma$ interactions beyond r_b , particles can be accelerated in the layers via first and second order Fermi processes, which constitute the origin of the GRB prompt emission. The internal shock stage lasts until the deceleration radius is reached, i.e. the distance where the interaction with the surrounding medium produces an external and a reverse shock.

In our model, the profile of the mean magnetic field follows a power-law shape, $B \propto r^{-\alpha}$ (see Appendix 1). The parameter that we consider as the less constrained is the intensity of the magnetic field at some point, either at the origin scale r_0 of a few gravitational radii, or at the beginning of the acceleration stage in the internal shocks at r_b . The other important index that controls the particle acceleration efficiency as a function of the particle energy is the index of the turbulent spectrum β (e.g. $\beta = 5/3$ for Kolmogorov theory). The efficiency of the Fermi acceleration process is directly related to the efficiency of particle scattering off magnetic irregularities. The most efficient acceleration is obtained with the so-called Bohm scaling, which corresponds to $\beta = 1$. This efficiency also scales with the level of magnetic irregularities $\eta_t \equiv \langle \delta B^2 \rangle / \langle B^2 \rangle$. In the following, we argue that the three parameters α , β and η_t can be determined by *Fermi* observations of GRB prompt emission, in particular through the measurement of the position of E_{peak} (i.e. the maximum of the νF_ν spectrum) and its evolution with time (see Appendix 1). More generally, the evolution of the synchrotron spectrum and the value of the maximum synchrotron emitted energy all simply depend on these three parameters.

2.2. Acceleration processes and characteristic time

The acceleration processes are all collisionless, and they mainly depend on the local magnetic field irregularities. In this paper, we do not hypothesize on the geometrical configuration of the magnetic field. We only assume an evolution profile for the magnetic field intensity, $B \propto r^{-\alpha}$ with $\alpha \in [1, 2]$, and the existence of a turbulent component. Following previous works (Gialis & Pelletier (2003)), we introduce a Kolmogorov turbulence spectrum such that

$$\langle \delta B^2 \rangle \propto \int_{k_{\min}}^{k_{\max}} k^{-5/3} dk, \quad (1)$$

where $k_{\min} \simeq 2\pi/\Delta R$. The upper bound k_{\max} is given by the cyclotron pulsation of the non-relativistic protons and the Alfvén speed: $k_{\max} \simeq \omega_{\text{cp}}/V_A$ with $\omega_{\text{cp}} = eB/m_p c$ and $0.1 c \lesssim V_A < c$. A particle of charge q , with an energy ϵ , can be scattered off by Alfvén waves only if its Larmor's radius, $r_L = \epsilon/|q|B$, is greater than $\sim 2\pi/k_{\max}$, thus a particle of mass m is accelerated only if its Lorentz factor is $\gtrsim \gamma_{\min} = (|q|/e)(m_p/m)(V_A/c)$ (Lacombe (1977)). We want to emphasize this theoretical estimate which is based on the physical description of the acceleration process in a turbulent magnetic field. A similar result is usually obtained by invoking the fraction of energy which is injected in the electronic population, though it is not well known (see e.g. Pe'er & Waxman (2004)). Also, thermal protons can be accelerated while electrons are injected in Fermi acceleration processes only if their Lorentz factors $\gtrsim 10^2$ to 10^3 .

The lower bound of the synchrotron energy spectrum, in the co-moving frame, corresponding to a minimal electronic Lorentz factor $\gamma_{e,\min}$ close to a few 10^2 , is thus given by

$$\epsilon_{\text{syn}}^{\text{low}} \simeq 0.29 \left(\frac{\gamma_{e,\min}}{400} \right)^2 \left(\frac{B_b}{10^5 \text{ G}} \right) \left(\frac{r}{r_b} \right)^{-\alpha} \text{ keV}. \quad (2)$$

However, in a mildly relativistic internal shock (with a Lorentz factor $\gamma_* \simeq 1.5$), electronic and hadronic temperatures, respectively T_e and T_p , are of the same order: $T_e \simeq T_p \simeq \gamma_* m_p c^2$. Since $\gamma_{e,\min} < m_p/m_e$, a large fraction of the electronic population is injected in the acceleration process when a slow cooling regime occurs (see Appendix 2). According to the Diffusive Shock Acceleration (DSA) theory (see e.g. Drury (1983), Blandford & Ostriker (1978), or Bell (1978)), we will assume that mildly relativistic internal shocks produce a power law energy distribution for the accelerated particles¹, with a density of particles per unit of energy $dn_p/d\epsilon \propto \epsilon^{-p}$, with $p \in [2, 3[$. Then, a thermal electronic distribution, with a maximum close to $\epsilon_{\min}^e = \gamma_{e,\min} m_e c^2$, is extended by such a power law distribution for $\epsilon > \epsilon_{\min}^e$.

Casse et al. (2002) (see also Gialis & Pelletier (2003)) showed that the characteristic acceleration time, which is proportional to the particle mean free path, mainly depends on both the particle rigidity and the magnetic turbulence level. For a Kolmogorov spectrum, it is given by

$$t_{\text{acc}} \simeq 6.6 \times 10^{-2} \frac{\bar{\ell}}{c}, \quad (3)$$

where the mean free path, $\bar{\ell}$, of a particle is given by

$$\bar{\ell} = \frac{r_L}{\eta_t} \left(\frac{r_L}{\ell_c} \right)^{-2/3}. \quad (4)$$

¹ However, we think that this power law could be modified by considering a continuous second order Fermi process in the shocked and/or unshocked layers.

In this last expression, we define $\ell_c \simeq \Delta R$, as the magnetic correlation length and, $\eta_t \equiv \frac{\langle \delta B^2 \rangle}{\langle B^2 \rangle}$, the magnetic turbulence level. At this point, it is important to stress the importance of the magnetic field intensity (via particle Larmor's radius), its evolution with the distance ($B \propto r^{-\alpha}$) and its turbulence level: these parameters are not only essential in the definition of the characteristic acceleration time t_{acc} which controls the efficiency of the acceleration process for both leptons and hadrons, but they also determine the magnetic confinement capabilities of the medium and, consequently, they play a key role in the problem of Ultra-High Energy Cosmic Ray generation.

2.3. Cut-off energy and electron cooling regimes

The upper bound of the energy distribution is obtained by comparing the local acceleration time t_{acc} with both the synchrotron cooling time, t_{syn} , and the co-moving dynamical time $t_{\text{dyn}} \simeq r/\eta c$. Here, we assume that other cooling processes, like e.g. the inverse Compton cooling for electrons, are negligible. Thus, according to the magnetic field evolution with the distance r , if $t_{\text{syn}} > t_{\text{dyn}}$ at r_b , the energy of particles is only limited by the expansion, during all the internal shock stage. Now, if $t_{\text{syn}} < t_{\text{dyn}}$ at r_b , the energy limitation follows two stages of evolution. For usual magnetic parameters, this last case seems to apply to the electronic population, as we will demonstrate below.

The electron energy distribution cut-off (see Appendix 1), due to the synchrotron cooling, can be written (in c.g.s units)

$$\epsilon_{\text{max}}^e \simeq 1.9 \times 10^7 \left(\frac{\kappa_0}{10} \right)^{-3/4} \eta^{1/2} (B_b r_b^\alpha)^{-5/4} r^{s_1}, \quad (5)$$

where $B_b \simeq 10^5$ G is the magnetic field intensity at r_b ($\simeq \eta^2 r_0$), the index $s_1 = (5\alpha - 2)/4$, and we define the turbulence parameter $\kappa_0 \simeq 2.2 \times 10^{-1}/\eta_t$. At the very beginning of the internal shock phase, we obtain an electronic maximal Lorentz factor close to 400. The corresponding cut-off energy of synchrotron photons at r_b , namely $\epsilon_{\text{b,syn}}^e$, does not depend on the index α of the magnetic field intensity:

$$\epsilon_{\text{b,syn}}^e \simeq 0.31 \left(\frac{\kappa_0}{10} \right)^{-3/2} \left(\frac{\eta}{100} \right)^{-1} \left(\frac{B_b}{10^5 \text{ G}} \right)^{-3/2} \left(\frac{r_0}{10^7 \text{ cm}} \right)^{-1} \text{ keV}, \quad (6)$$

in the co-moving frame. The observational signature of such a cut-off energy could be observed at the very beginning of the prompt emission where the instantaneous electronic synchrotron spectrum could lie in a narrow energy band (10 - 100 keV) for a terrestrial observer. It is noteworthy that this cut-off energy is also independent of η in the observer frame. Finally, because $\epsilon_{\text{syn}}^{\text{low}}$ at r_b has to be $\leq \epsilon_{\text{b,syn}}^e$, we obtain a strong constraint on the upper bound of the magnetic field intensity B_b :

$$B_b \lesssim 1.0 \times 10^5 \left(\frac{\kappa_0}{10} \right)^{-3/5} \left(\frac{r_0}{10^7 \text{ cm}} \right)^{-2/5} \left(\frac{\gamma_{\text{e,min}}}{400} \right)^{-4/5} \left(\frac{\eta}{100} \right)^{-2/5} \text{ G}, \quad (7)$$

or, for the turbulence parameter,

$$\kappa_0 \lesssim 10 \left(\frac{B_b}{10^5 \text{ G}} \right)^{-5/3} \left(\frac{r_0}{10^7 \text{ cm}} \right)^{-2/3} \left(\frac{\gamma_{\text{e,min}}}{400} \right)^{-4/3} \left(\frac{\eta}{100} \right)^{-2/3}. \quad (8)$$

From Eq. (7), we deduce that only high magnetic field intensity ($B_b \gtrsim 10^5$ G) requires an high turbulence level (i.e. $\kappa_0 \simeq 10$, see above). Thus, because the magnetic field at r_b can vary from 10^3 to 10^7 G depending on the magnetic properties of the central engine, one has to consider different levels of turbulence when studying particle acceleration processes in the internal shocks (see Sec. 3).

The evolution of the cut-off energy of synchrotron photons, with the distance r and beyond r_b , is given by

$$\epsilon_{\text{syn}}^{\text{max}} = \epsilon_{\text{b,syn}}^e \left(\frac{r}{r_b} \right)^{2s_1 - \alpha}. \quad (9)$$

Eq. (9) is valid until what we could name the ‘‘cooling radius’’ r_c , where the co-moving dynamical time becomes shorter than the cooling synchrotron time. The cooling radius is such that

$$r_c \simeq \left(1.0 \times 10^{-24} \left(\frac{\kappa_0}{10} \right)^{-3} \eta^{-2} (B_b r_b^\alpha)^3 \right)^{\frac{1}{3\alpha - 2}} \text{ cm}. \quad (10)$$

The variations of this radius with the magnetic parameters α , B_b , and κ_0 are strong important (see Fig. 1). For example, on one hand, no transition occurs for an index α close to 1 and for a high turbulence level ($\kappa_0 \simeq 10$): the synchrotron limitation prevails and the cooling radius is moved away beyond the deceleration radius, namely r_d . On the other hand, for a low turbulence level ($\kappa_0 \geq 100$) with $\alpha > 1.5$, the cooling radius is smaller than r_b and the limitation is only due to expansion.

Beyond the cooling radius, and until the deceleration radius, the cut-off energy of the electronic distribution is (in c.g.s units)

$$\epsilon_{\text{max}}^e \simeq 1.9 \times 10^{-11} \left(\frac{\kappa_0}{10} \right)^{-3} \eta^{-1} B_b r_b^\alpha r^{s_2}, \quad (11)$$

with the index $s_2 = 1 - \alpha$. Thus, we obtain a new evolution for the cut-off energy with the distance r , and beyond r_c :

$$\epsilon_{\text{syn}}^{\text{max}} = \epsilon_{\text{c,syn}}^e \left(\frac{r}{r_c} \right)^{2s_2 - \alpha}. \quad (12)$$

In Appendix 2, we detail the calculation of the electronic synchrotron spectrum which is locally produced at the distance r , by taking into account both the previous cut-off energy and the variation of the electronic cooling regime.

In the co-moving frame, and at the cooling radius r_c , the cut-off energy of the corresponding synchrotron spectrum only depends on the turbulence level. Indeed, Eq. (9) and (10) yield

$$\epsilon_{\text{c,syn}}^e \simeq 10 \left(\frac{\kappa_0}{10} \right)^{-3} \text{ MeV}. \quad (13)$$

The energy $\epsilon_{\text{c,syn}}^e$ is now considered as the cut-off energy of the whole electronic synchrotron spectrum (Gialis & Pelletier 2005) when one neglects absorption processes like e.g. γ - γ interactions (see Sec. 3). A direct observation of its spectral signature, in the GeV range, would provide a very good estimate of the turbulence level. Moreover, as suggested by Eq. (10) and by the Fig. 1, the determination of the duration separating the very beginning of the prompt emission and the observation of the highest energy synchrotron photons, i.e $\Delta t \simeq (r_c - r_b)/\eta^2 c$ for a terrestrial observer, could constitute a very interesting observational test to constrain the index α of the magnetic field evolution law in the outflow. Sec. 3 will examine the possible absorption of high energy photons in γ - γ interactions with the lower energy photons.

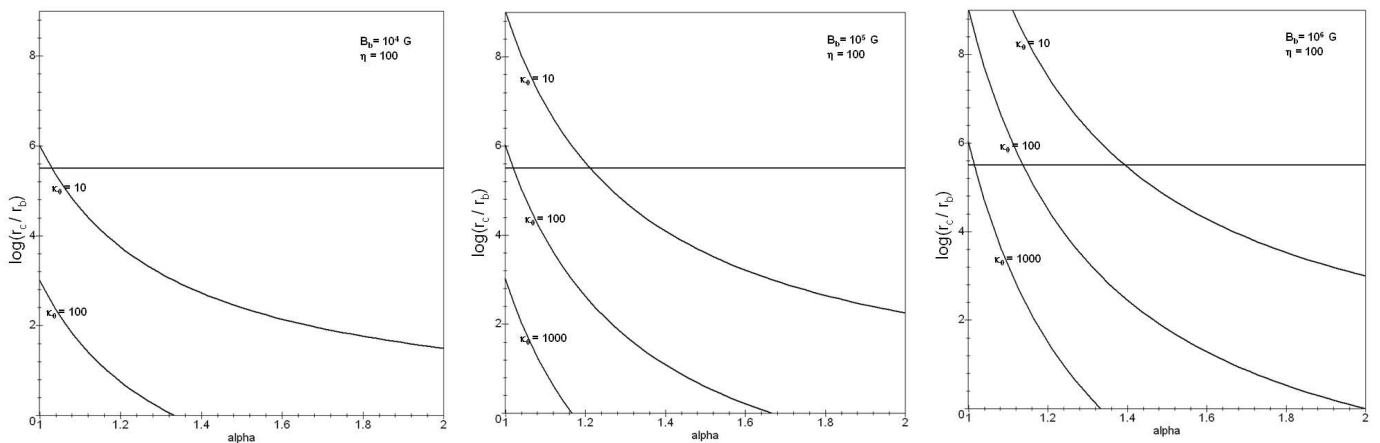


Fig. 1. Variation of the cooling radius r_c with the magnetic field intensity, the turbulence level and the index α . The horizontal line corresponds to about the deceleration radius i.e the end of the internal shock stage.

3. Pair production process and high energy cut-off in synchrotron spectrum

In the internal shock stage of GRBs, the highest energy synchrotron photons can interact with lower energy photons to create some e^+e^- pairs. The resulting absorption can prevent any observational signature, in the synchrotron spectrum, of an high energy cut-off in the electronic distribution. In this section, we will assume that effects from a possible Compton Inverse process are negligible, which holds for magnetic dominated GRB outflows.

3.1. General considerations

Many studies of pair production process have been made (see e.g. Granot et al. (2008)) in GRB internal shock model, but the evolution of the magnetic field during the expansion is not generally taking into account. Indeed, the threshold energy of this process is very dependent on the magnetic field parameters. We propose here an analytical estimation of pair production effects by using our previous results concerning the synchrotron spectrum and its evolution with time. We consider a possible interaction of a photon having a high energy ϵ_h with a photon having a lower energy ϵ_ℓ . These energies will be expressed in the co-moving frame. The cross section depends on the angle θ between their directions of propagation. Then, the cross section is given by (Gould & Schröder (1967))

$$\sigma_{\gamma\gamma}(\epsilon_h, \epsilon_\ell, \mu) \simeq \frac{3}{16} \sigma_T (1 - \beta^2) \left[(3 - \beta^4) \ln \left(\frac{1 + \beta}{1 - \beta} \right) - 2\beta(2 - \beta^2) \right], \quad (14)$$

where

$$\beta = \left(1 - \frac{2(m_e c^2)^2}{(1-\mu)\epsilon_h\epsilon_\ell} \right)^{1/2}, \quad (15)$$

and $\mu = \cos\theta$.

The threshold energy for this interaction is such that

$$\epsilon_{\text{th}} = \frac{2(m_e c^2)^2}{(1-\mu)\epsilon_h}, \quad (16)$$

and $\sigma_{\gamma\gamma}$ is maximal for $\beta = \sqrt{2}/2$: $\sigma_{\gamma\gamma}^{\text{max}} \simeq 0.26 \sigma_T$. In our case, the co-moving threshold energy depends on r and, for the highest energy photons (see Eq. (9) and (12)), we have

$$\epsilon_{\text{th}}(r) = \begin{cases} \frac{2(m_e c^2)^2}{(1-\mu)\epsilon_{\text{b,syn}}^e} \left(\frac{r}{r_b} \right)^{\alpha-2s_1} & \text{for } r_b \leq r \leq r_c \\ \frac{2(m_e c^2)^2}{(1-\mu)\epsilon_{\text{c,syn}}^e} \left(\frac{r}{r_c} \right)^{\alpha-2s_2} & \text{for } r \geq r_c \end{cases}. \quad (17)$$

At r_c , for $\kappa_0 = 10$ and for a head-on interaction ($\mu = -1$), $\epsilon_{\text{th}} \simeq 26$ keV in the co-moving frame, and whatever α . For a sufficient low energy photon density, the highest energy photons can create pairs only when $\epsilon_{\text{th}}(r) \leq \epsilon_{\text{syn}}^{\text{max}}$ i.e between the radii

$$r_{\text{th,min}} = \left(\frac{m_e c^2}{\epsilon_{\text{b,syn}}^e} \right)^{\frac{1}{2s_1-\alpha}} r_b, \quad (18)$$

and

$$r_{\text{th,max}} = \left(\frac{m_e c^2}{\epsilon_{\text{c,syn}}^e} \right)^{\frac{1}{2s_2-\alpha}} r_c, \quad (19)$$

with $r_c \in [r_{\text{th,min}}, r_{\text{th,max}}]$. As illustrated in the Fig. 2, these radii are relevant only for a set of magnetic parameters: for example, for α close to 1, there is no possibility of γ - γ absorption. This is a specific case where the cut-off in the electronic distribution could have an observational signature (see Fig. 3), only if the turbulence is weak enough ($\kappa_0 \gg 10$). For a higher turbulence level ($\kappa_0 \lesssim 10$), this cut-off could only be observable for $\alpha \gtrsim 1.2$ (i.e when $r_c < r_d$).

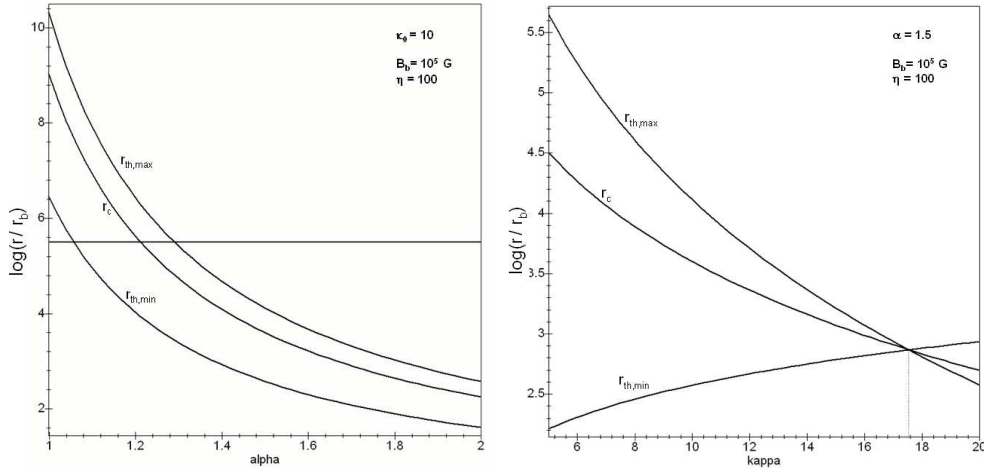


Fig. 2. Left: Variation of the threshold radii with the index α for an usual turbulence level. The horizontal line corresponds to a distance of about the deceleration radius i.e the end of the internal shock stage. Right: Variation of the threshold radii with the turbulence level for $\alpha = 1.5$.

When the γ - γ absorption is possible, i.e when $r_{\text{th,min}} < r_d$, we have to examine the cut-off energy in the synchrotron spectrum. For a high energy photon, the mean free path, $\ell_{\gamma\gamma}(\epsilon_h)$, is such that

$$\ell_{\gamma\gamma}^{-1}(\epsilon_h) = \frac{1}{2} \int_{-1}^1 d\mu (1-\mu) \int_{\epsilon_{\text{th}}}^{\epsilon_{\text{syn}}^{\text{max}}} \sigma_{\gamma\gamma}(\epsilon_h, \epsilon_\ell, \mu) \frac{dn_\gamma(\epsilon_\ell)}{d\epsilon_\ell} d\epsilon_\ell, \quad (20)$$

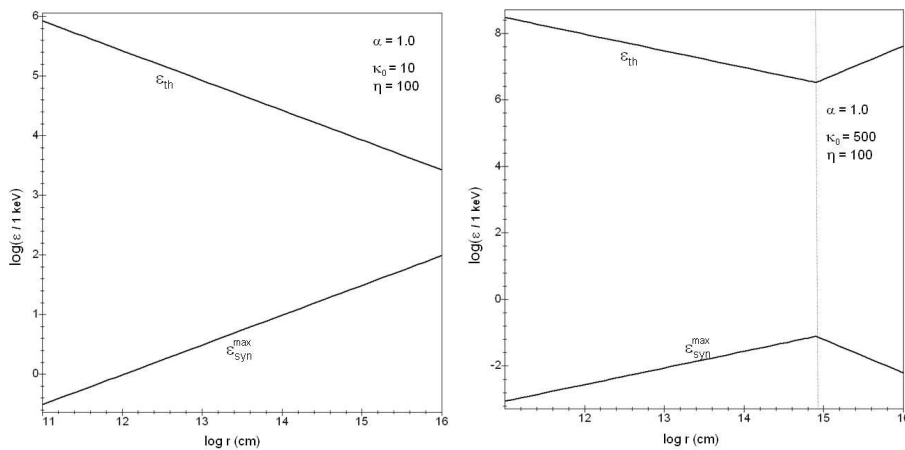


Fig. 3. The case $\alpha = 1.0$ (i.e $B \propto r^{-1}$) with $B_b = 10^5$ G: comparison of the maximum energy (co-moving) of synchrotron photons with the corresponding threshold energy of the pair creation process, for two different turbulence levels. No pair creation process is possible.

where $n_\gamma(\epsilon_\ell)$ is the number of photons per cm^{-3} at the energy ϵ_ℓ .

Following Gould & Schröder (1967), we introduce $s = \epsilon_\ell/\epsilon_{th} = s_0 \Theta$, with $\Theta = \frac{1}{2}(1 - \mu)$ and, $s_0 = \epsilon_\ell \epsilon_h / (m_e c^2)^2$. Thus, we can write

$$\ell_{\gamma\gamma}^{-1}(\epsilon_h) = \frac{3}{8} \sigma_T \left(\frac{m_e^2 c^4}{\epsilon_h} \right)^2 \int_{\frac{m_e^2 c^4}{\epsilon_h}}^{\infty} \epsilon_\ell^{-2} \frac{dn_\gamma(\epsilon_\ell)}{d\epsilon_\ell} d\epsilon_\ell \int_1^{s_0(\epsilon_\ell)} s \bar{\sigma}(s) ds, \quad (21)$$

with $\bar{\sigma}(s) \simeq \frac{16}{3} \frac{\sigma_{\gamma\gamma}}{\sigma_T} \simeq 1$ if $s \gtrsim 1$, and $\bar{\sigma}(s) \simeq \ln(s)/s$ if $s \gg 1$. Also, we can define the internal optical depth, namely $\tau_{\gamma\gamma}(\epsilon_h, r)$, as the ratio between the co-moving dynamical time, t_{dyn} , and the mean time between two pair production interactions, i.e $\ell_{\gamma\gamma}(\epsilon_h)/c$.

3.2. Absorption estimate in GRB outflows

Considering now that the resulting photon distribution, in the outflow and expressed in the co-moving frame, is well described by a Band's function (Band et al. (1993)), we have²:

$$\frac{dn_\gamma}{d\epsilon_\ell} \simeq K \frac{\eta L_\gamma^{\text{iso}} \Delta t_w}{4\pi r^2 \Delta R E_{\text{peak}}^2} F\left(\frac{\eta \epsilon_\ell}{E_{\text{peak}}}\right), \quad (22)$$

where $E_{\text{peak}} (\simeq 100 \text{ keV})$ is the energy for which the observed νF_ν spectrum is maximum, $L_\gamma^{\text{iso}} \simeq 10^{51} \text{ erg}\cdot\text{s}^{-1}$ is the observed isotropic γ -ray luminosity and,

$$F(x) = \begin{cases} x^{\alpha_B} \exp(-(2 + \alpha_B)x) & \text{for } x \leq x_0 \\ x^{\beta_B} x_0^{\alpha_B - \beta_B} \exp(-(2 + \alpha_B)x_0) & \text{for } x \geq x_0 \end{cases}, \quad (23)$$

with $x_0 = (\alpha_B - \beta_B)/(2 + \alpha_B)$, and the normalization constant $K = (\int x F(x) dx)^{-1}$. The Band's parameters, α_B and β_B , depend on the GRB and, their mean values are close to -1 and -2.2 respectively (Preece et al. (2000)). Moreover, following the previous section, the resulting photon distribution could exhibit a cut-off energy at $\epsilon_{c,\text{syn}}^e$. Assuming that $\sigma_{\gamma\gamma} \simeq \sigma_{\gamma\gamma}^{\text{max}}$, and that γ - γ interactions occur only at the threshold energy:

$$\ell_{\gamma\gamma}^{-1}(\epsilon_h) \simeq 0.26 \sigma_T \int_0^{\epsilon_{c,\text{syn}}^e} \epsilon_\ell \delta(\epsilon_\ell - \epsilon_{th}) \frac{dn_\gamma}{d\epsilon_\ell} d\epsilon_\ell, \quad (24)$$

where $\epsilon_{th} \simeq (m_e c^2)^2/\epsilon_h$, and δ , Dirac's function. Then, in the co-moving frame, we deduce the internal optical depth

$$\tau_{\gamma\gamma}(\epsilon_h, r) \simeq K \frac{0.26 \sigma_T \eta L_\gamma^{\text{iso}} \Delta t_w (m_e c^2)^2}{4\pi r^2 E_{\text{peak}}^2 \epsilon_h} F\left(\frac{\eta (m_e c^2)^2}{E_{\text{peak}} \epsilon_h}\right). \quad (25)$$

At the distance r , this expression is valid only for photons with an energy $\epsilon_h > \epsilon_m \simeq m_e^2 c^4 / \epsilon_{\text{syn}}^{\text{max}}$, the minimal energy threshold. The energy of cut-off, namely ϵ_{cut} , is defined by $\tau_{\gamma\gamma}(\epsilon_{\text{cut}}, r) = 1$ for $\epsilon_{\text{cut}} > \epsilon_m$.

² We neglect corrections due to cosmological redshift.

The possibility to have an observational signature, in the synchrotron spectrum, of the cut-off energy relating to the electronic distribution, is determined by both the choice of the magnetic parameters (turbulence level, index α and intensity B_b) and the duration Δt_w and/or the luminosity of the bursts. As it is illustrated, for example, on Fig. 4 and 5, for high turbulence level, the γ - γ absorption could only occur during a short while around r_c comparing to the internal shock phase duration. We could thus distinguish two situations: first, when $\epsilon_{\text{cut}} > \epsilon_{c,\text{syn}}^e$ at the distance r_c , we could directly observe the photons with the highest cut-off energy, $\epsilon_{c,\text{syn}}^e$, and obtain the occurring date of this maximum (see Sec. 2.3). When $\epsilon_{\text{cut}} < \epsilon_{c,\text{syn}}^e$ around r_c , we could deduce $\epsilon_{c,\text{syn}}^e$ by determining the slopes ($2s_1 - \alpha$ and $2s_2 - \alpha$, see Eq. (9) and (12)) of the evolution, with time, of the cut-off energy in the photon spectrum when there is no γ - γ absorption i.e during the largest part of the internal shock stage. It is important to note that the original observational test that we propose here, is only based on the observation of the cut-off energy of the resulting synchrotron spectrum which evolves during all the internal shock phase: in fact, we don't need to observe the precise shape of the spectrum. In both cases, observations by *Fermi* observatory could easily constrain magnetic parameters.

Finally, for a low turbulence level ($\kappa_0 > 100$), the γ - γ absorption does not affect the synchrotron spectrum (see Fig. 6), but the highest cut-off energy of the electronic distribution, can yield an observational signature at r_b : according to Eq. (11), it is noteworthy that this cut-off energy at r_b is not dependent on the index α , and does not correspond to any transition between two different energy limitations (i.e r_c). However, because of a too strong adiabatic cooling (see Eq. (7) and (8)), this situation would be incompatible with the acceleration process in the internal shocks: indeed, this process could not simply start.

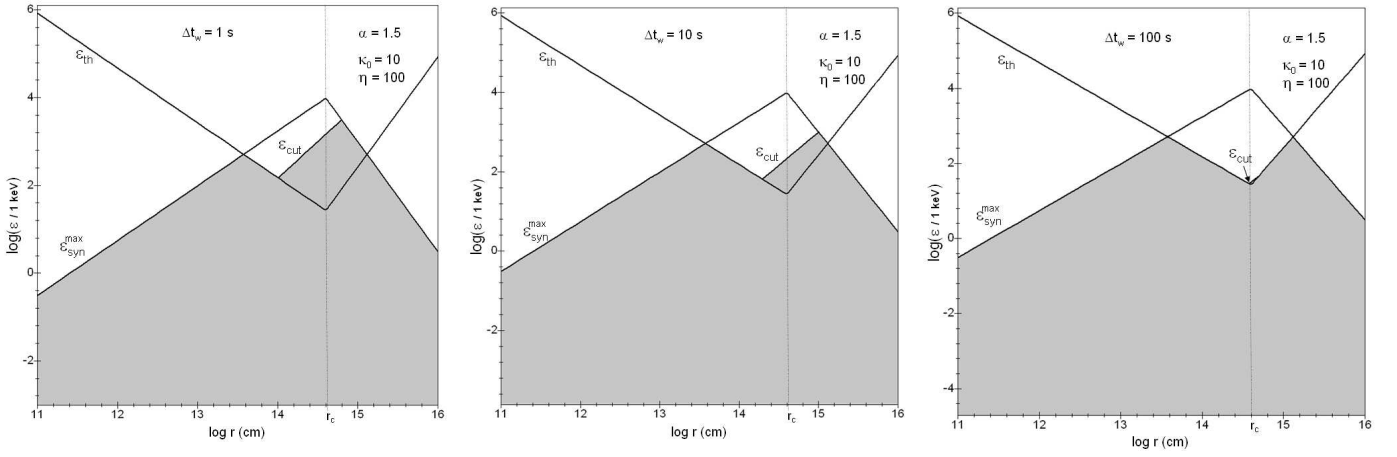


Fig. 4. The case $\alpha = 1.5$ (i.e $B \propto r^{-3/2}$) with $B_b = 10^5 \text{ G}$, $E_{\text{peak}} = 100 \text{ keV}$, $\alpha_B = -1$ and $\beta_B = -2.2$, for different burst durations Δt_w : comparison of the maximum energy (co-moving) of synchrotron photons with the corresponding threshold energy of the pair creation process ($\epsilon_{\text{th}} = \epsilon_m$), and the cut-off energy ϵ_{cut} . The upper boundary of the grey zone is the energy of the highest synchrotron photons which are observable. For a high turbulence level, the γ - γ absorption is important, and the cut-off relating to the electronic distribution, at r_c , is unobservable.

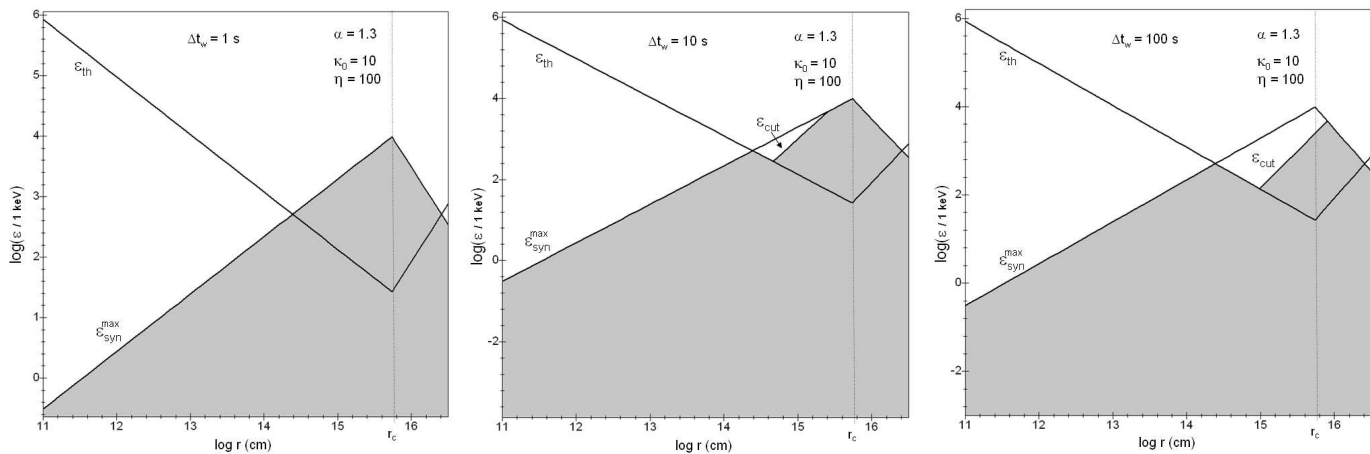


Fig. 5. The case $\alpha = 1.3$ (i.e. $B \propto r^{-1.3}$) with $B_b = 10^5$ G, $E_{\text{peak}} = 100$ keV, $\alpha_B = -1$ and $\beta_B = -2.2$, for different burst durations Δt_w : comparison of the maximum energy (co-moving) of synchrotron photons with the corresponding threshold energy of the pair creation process ($\epsilon_{\text{th}} = \epsilon_m$), and the cut-off energy ϵ_{cut} . The upper boundary of the grey zone is the energy of the highest synchrotron photons which are observable. For a high turbulence level, the γ - γ absorption is important only for very long bursts, and the cut-off relating to the electronic distribution, at r_c , could be easily observable.

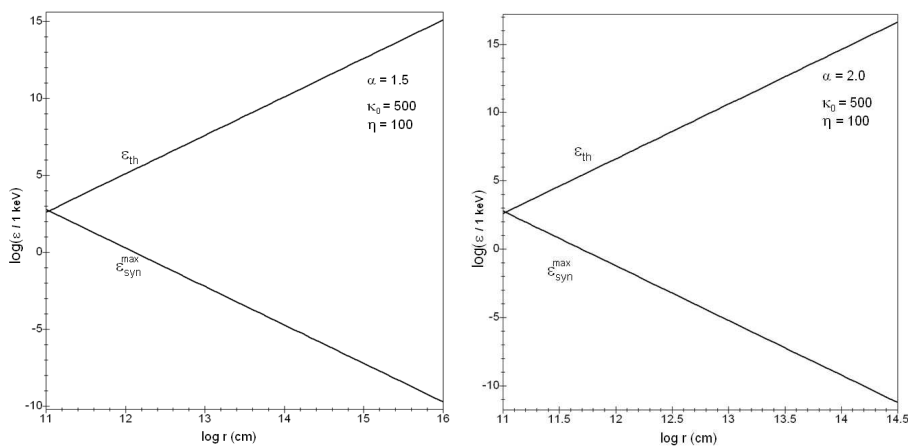


Fig. 6. Comparison of the maximum energy (co-moving) of synchrotron photons with the corresponding threshold energy of the pair creation process ($\epsilon_{\text{th}} = \epsilon_m$) for a low turbulence level, and for $B_b = 10^5$ G: there is no γ - γ absorption.

4. Synchrotron emission from UHECRs

In the previous section, we focused on the electronic population. Here, we intend to study the possibility of an observational signature of Ultra-High Energy Cosmic Rays (UHECRs), produced in the internal shocks, via their synchrotron emission. In fact, we want to determine on which conditions the synchrotron photons from accelerated protons and, more particularly, from UHECRs, could be distinguished from leptonic synchrotron and SSC components, without undergoing γ - γ absorption.

4.1. Efficiency of UHECR acceleration processes

Following our previous works (Gialis & Pelletier (2003), and Gialis & Pelletier (2004)), let us first consider the energy of the accelerated protons resulting from usual Fermi's process, as described at the very beginning of Sec. 2: because $t_{\text{syn}} > t_{\text{dyn}}$ at r_b , we deduce that the only energy limitation results from the expansion³. Also, contrary to electrons, protons undergo a single cooling regime during all the expansion: the slow one (see Appendix 2). Then, the energy distribution of protons is such that $dn_p/d\epsilon \propto \epsilon^{-p}$, with $p \in [2, 3]$, between $\epsilon_0 \simeq 1$ GeV and, ϵ_{max}^p , the highest energy that protons can achieve in the co-moving frame. According to Eq. (11) and with $r_b \simeq \eta^2 r_0$, we have

$$\epsilon_{\text{max}}^p \simeq 1.2 \times 10^6 \left(\frac{\kappa_0}{10}\right)^{-3} \left(\frac{\eta}{100}\right) \left(\frac{r_0}{10^7 \text{ cm}}\right) \left(\frac{B_b}{10^5 \text{ G}}\right) \left(\frac{r}{r_b}\right)^{s_2} \text{ GeV}, \quad (26)$$

³ We assume that the outflow is always transparent to p - p interactions beyond a few r_b (see Gialis & Pelletier (2003)), and we neglect proton energy losses due to p - γ interactions.

with the index $s_2 = 1 - \alpha$. This is the same energy limitation as for electrons, because it depends only on the charge of the particle, and not on its mass. Whatever any reasonable magnetic parameters, it shows that protons cannot achieve the UHECR energy range⁴, by considering a such scenario for Fermi's process, as it was suggested by Waxman (1995).

To produce UHECRs, a secondary acceleration process is required. As it has been proposed by Gialis & Pelletier (2004), the protons, pre-accelerated in the internal shocks, could be scattered off multiple magnetized fronts, the internal shocks themselves, and could undergo a kind of "second order" Fermi process, which is efficient in this mildly relativistic regime.

The scenario is the following one: each internal shock can be described as a magnetized front in the resulting shocked layer. These magnetized fronts can propagate in both opposite directions in the co-moving frame. Thus, protons are not only accelerated by diffusion process on both sides of the internal shocks, but they can also undergo an acceleration mechanism directly by reflection or scattering off the mildly relativistic magnetized fronts. Also, at each scattering, the cosmic rays have an energy gain of order γ_*^2 , where $1 < \gamma_* \lesssim 2$ is the average relative Lorentz factor of a front in the co-moving frame. Because of the magnetic field strength and the relativistic expansion of the layer width, the accelerated protons could be confined in their initial layer, until they reach the local confinement energy limit, given by Hillas' criterium. Because of the anisotropy of their angular distribution function, the particles could mainly escape downstream or upstream of their layer, and consequently stay in the relativistic flow. Then, cosmic rays can be accelerated again, out of their initial layer, when they encounter other magnetized layers. As we have previously seen in a Monte-Carlo simulation (Gialis & Pelletier (2004)), the escaping probability out of the collimated wind flow is weak enough during the acceleration stage from r_b to a few hundreds of r_b .

This secondary acceleration process could be efficient to produce UHECRs: the reason is that the characteristic acceleration time of this process is of the order of the time separating two layer collisions, which is much smaller than the synchrotron cooling time, t_{syn} , and the dynamical time, t_{dyn} , for a sufficient number of layers, namely N_s . Let us write this acceleration time, in the co-moving frame, for a flow with $N_s \gg 1$;

$$t_{\text{acc}} \simeq \frac{L_{\text{com}} - N_s \Delta R}{c N_s} \simeq m t_{\text{dyn}}, \quad (27)$$

where $L_{\text{com}} = c \Delta t_w r / \eta r_0$ is the co-moving length of the flow, $\Delta R = r / \eta$, the width of a layer, and

$$m = \frac{c \Delta t_w}{N_s r_0} - 1. \quad (28)$$

Assuming that $0.5 N_s^{\text{max}} < N_s < N_s^{\text{max}}$, with $N_s^{\text{max}} = c \Delta t_w / r_0$, we deduce that $0 < m < 1$.

Writing $\dot{\epsilon} \simeq \epsilon / t_{\text{acc}}$, for a particle of energy ϵ , we obtain the time for which, a particle, with an initial energy ϵ_0 at t_0 , achieve an energy ϵ ;

$$t = t_0 \left(\frac{\epsilon}{\epsilon_0} \right)^m < t_0 \left(\frac{\epsilon}{\epsilon_0} \right). \quad (29)$$

Consequently, a proton with $\epsilon_0 \simeq 10^6$ GeV (see Eq. (26)), at a few r_b , achieve the UHECR energy range ($\epsilon = 10^8$ GeV) at the time $t \lesssim 10^2 t_b$, in the co-moving frame, where $t_b = r_b / \eta c$. At last, it is interesting to mention that the characteristic time, $t_{p\gamma}$, of p- γ interaction cooling is such that $t_{p\gamma} / t_{\text{acc}} \gtrsim r / r_b$ for $r > r_b$: thus, we can neglect this cooling process for UHECRs, even if a resulting high energy neutrino emission may be possible (Gialis & Pelletier (2003)).

Numerical simulations showed that such an acceleration process extends the energy distribution of protons until the local confinement energy limit, i.e $\epsilon_{\text{cl}} \simeq e B \Delta R$. Then, the corresponding cut-off energy for synchrotron photons, produced by these UHECRs, is

$$\epsilon_{\text{p,syn}}^{\text{max}} \simeq 1.0 \left(\frac{\eta}{100} \right)^2 \left(\frac{r_0}{10^7 \text{ cm}} \right)^2 \left(\frac{B_b}{10^5 \text{ G}} \right)^3 \left(\frac{r}{r_b} \right)^{2s_2 - \alpha} \text{ GeV}, \quad (30)$$

in the co-moving frame. However, according to the acceleration process, UHECRs cannot be produced before a few tens of r_b . Also, because of the magnetic field decrease, the emitted synchrotron photons will have a lower energy, and the energy cut-off of these photons would be equal to a few tens of MeV in the co-moving frame, i.e a few GeV for a terrestrial observer, for α close to 1. In fact, the energy range of the hadronic synchrotron peak is very sensitive to the index α of the magnetic field decrease (see Fig. 7): from Eq. (9) and (30), and for a dominant leptonic emission (see Sec. 4.2), we deduce that synchrotron signature of UHECRs would be compromised for a magnetic field evolution very different from $B \propto r^{-1}$. For this reason, hereafter, we will assume an index α very close to 1.

⁴ Particles with an energy $\geq 10^8$ GeV in the co-moving frame.

4.2. Comparison between hadronic and leptonic synchrotron emissions

First, we examine observability of an UHECR synchrotron component by comparing the hadronic and leptonic luminosities. Their ratio can be simply expressed by

$$\frac{L_{\text{syn}}^{\text{p}}}{L_{\text{syn}}^{\text{e}}} = \left(\frac{m_e}{m_p}\right)^2 \frac{N_p \langle \gamma_p^2 \rangle}{N_e \langle \gamma_e^2 \rangle}, \quad (31)$$

where N_p and N_e are the numbers of emitting particles and, γ_p and γ_e their Lorentz factors. In the case of non-relativistic shocks, we could have $N_p \gg N_e$, but no generation of UHECRs would be possible in our Fermi acceleration scenario. The situation is quite different in mildly relativistic internal shocks: in fact, because of a higher temperature (see Sec. 2.2), a large fraction of the electronic population is injected in the acceleration process and then, produce an higher synchrotron emission. Also, in Eq. (31), we can assume $N_p \simeq N_e$. For energy distributions $\propto \gamma^{-2}$, inserting Eq.(5), we obtain

$$\frac{L_{\text{syn}}^{\text{p}}}{L_{\text{syn}}^{\text{e}}} \simeq \left(\frac{m_e}{m_p}\right)^2 \frac{\gamma_{\text{p,min}} \gamma_{\text{p,max}}}{\gamma_{\text{e,min}} \gamma_{\text{e,max}}} \simeq 1.8 \times 10^{-3} \left(\frac{\gamma_{\text{e,min}}}{400}\right)^{-2} \left(\frac{r}{r_b}\right)^{-s_1}, \quad (32)$$

in the synchrotron cooling stage ($r < r_c$). An hadronic synchrotron component seems to be undetectable. However, for α close to 1, the energy range of hadronic and leptonic components are very different around the distance ($\sim 100 r_b$) where the UHECR population is formed: indeed, $r_c \gg 100 r_b$ and the cut-off energy for hadronic and leptonic synchrotron components are respectively around a few GeV and a few hundreds of keV for a terrestrial observer (see Fig. 7). Thus, because this emission would begin around a few hundreds of t_b/η , i.e a few tens of ms after the very beginning of the prompt emission, in the observer frame, hadronic synchrotron photons could be detectable if one can observe the evolution of the spectrum with time as it was previously suggested in Sec. 3.2.

4.3. SSC and pair creation effects on observability

Concerning a possible pair creation process, the energy of threshold, for this synchrotron photons, is

$$\epsilon_{\text{th}}^{\text{p}} \simeq \frac{(m_e c^2)^2}{\epsilon_{\text{p,syn}}^{\text{max}}} \simeq 2.6 \times 10^{-1} \left(\frac{\eta}{100}\right)^{-2} \left(\frac{r_0}{10^7 \text{ cm}}\right)^{-2} \left(\frac{B_b}{10^5 \text{ G}}\right)^{-3} \left(\frac{r}{r_b}\right)^{\alpha-2s_2} \text{ keV}, \quad (33)$$

beyond $\sim 100 r_b$. Thus, for α close to 1, there is no γ - γ absorption, because $\epsilon_{\text{th}}^{\text{p}}$ is always $\gg \epsilon_{\text{syn}}^{\text{max}}$, the cut-off energy of the electronic synchrotron spectrum, whatever the distance r (see Fig. 8).

Let us now investigate the possible obstacle to the observation of the synchrotron emission of UHECRs due to the SSC emission. This depends on the Compton parameter $Y \equiv U_s/U_B$, i.e the ratio between the energy densities of the synchrotron radiation and of the magnetic field. Indeed, the synchrotron spectrum is Comptonized such that a second bump at few 100 MeV range is generated (see below); its luminosity peak is almost the synchrotron luminosity peak multiplied by Y . Actually the real parameter is weakened by the Klein-Nishina regime, which mostly amounts to multiply Y by the fraction of soft photons of energy below the threshold of pair creation. Anyway this does not change the order of magnitude. However, the synchrotron spectrum is not simply duplicate; its high energy part decays more rapidly (its index is more or less increased by 1). Nevertheless, this SSC emission can totally hide the high energy cut-off of the leptonic synchrotron spectrum for $Y \gtrsim 10^{-2}$, unfortunately; and thus we cannot determine directly the electron distribution cut-off. But an indirect determination is not excluded, as explained previously when discussion about the γ - γ absorption (see 3.2).

The dominant electronic population has a Lorentz factor $\bar{\gamma}_e \lesssim 10^3$ during all the expansion, and, in the outflow, the most important photon field corresponds to the E_{peak} i.e photons with energy $\epsilon_{\text{peak}} \simeq \text{few keV}$ in co-moving frame. Thus, the SSC-peak is estimated around 100 MeV ($\simeq \eta \bar{\gamma}_e^2 \epsilon_{\text{peak}}$ in terrestrial observer frame), and the hadronic synchrotron spectrum could be observed around a few GeV as predicted above, provided that the Compton parameter Y be sufficiently small ($< 10^{-2}$), which is consistent with the requirement of a magnetic dominated outflow suitable for UHECR generation (see also, e.g., Asano & Inoue (2007)).

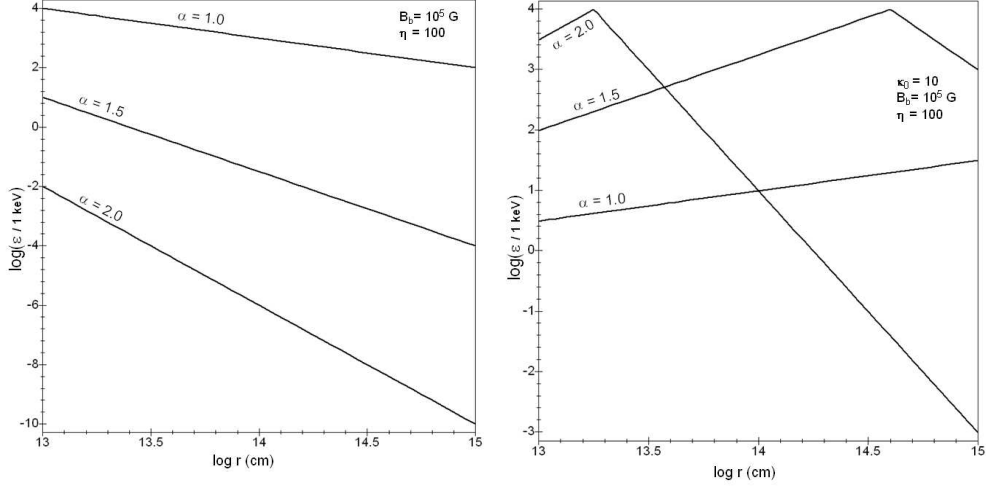


Fig. 7. Comparison of the cut-off energy, $\epsilon_{p,\text{syn}}^{\text{max}}$, of the UHECR synchrotron spectrum (left), with the cut-off energy, $\epsilon_{\text{syn}}^{\text{max}}$, of the electronic synchrotron spectrum (right), for different magnetic index α , and in the co-moving frame.

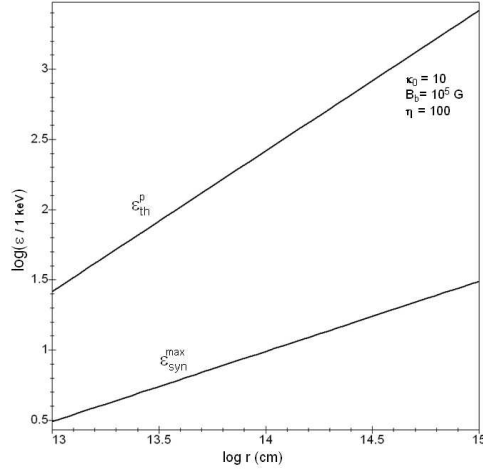


Fig. 8. Comparison of the threshold energy, ϵ_{th}^p , with the cut-off energy, $\epsilon_{\text{syn}}^{\text{max}}$, of the electronic synchrotron spectrum, for $\alpha = 1$, and in the co-moving frame. There is no possible γ - γ absorption.

5. Discussion and conclusion

The analysis we have made allows to draw several unexpected conclusions about a possible diagnosis of magnetic field parameters (turbulence level, index α and intensity B_t) and particle acceleration processes in the internal shock stage, by taking the observational limitations due to γ - γ absorption and SSC process into account. We proposed to estimate these magnetic field parameters by studying some observational consequences of their variations and, more particularly, by determining the evolution of the cut-off energy of the synchrotron part of the electronic spectrum. We then detailed on which conditions the signatures of accelerated leptonic and hadronic population of particles could be observed during the GRB prompt emission.

Let us summarize our results:

- First, we show that the electronic synchrotron spectrum which can be observed at the very beginning of the internal shock phase by *Fermi* observatory could lie in a narrow energy band (10-100 keV) for a terrestrial observer. Moreover, the cut-off energy of this spectrum places constraints upon both magnetic field intensity and its turbulence level, that we determined (see Eq. (7) and (8)).
- For a magnetic field ($B \propto r^{-\alpha}$) with an index $1 \leq \alpha \lesssim 1.2$ and by considering an high level of magnetic field turbulence ($\eta_t \simeq 10^{-2}$), we cannot observe any highest cut-off energy in the electronic synchrotron spectrum, corresponding to $\epsilon_{\text{c,syn}}^e$, because the cooling radius, r_c , would be too far from the inner engine. In another hand, this case would be the most favourable to observe an early high energy synchrotron signature from UHECRs, with a cut-off energy around a few GeV, on the condition that there is no too strong SSC component in this energy range (in fact, when $Y < 10^{-2}$), in the internal shocks at the same moment. It is noteworthy that the magnetic field

decreases in $1/r$ in two important cases: one case corresponds to the existence of a large scale mean field anchored in a central rotator (this is then a toroidal field that dominates at large distance), the other case corresponds to the amplification of the magnetic field to equipartition at each shock ($P_{mag} \sim P \sim \rho \gamma_* c^2$ with $\rho \propto 1/r^2$).

- For $1.2 \lesssim \alpha \lesssim 1.4$, the electronic synchrotron spectrum could reveal an highest cut-off energy just before the end of the prompt emission, despite the pair creation process with gamma photons of lower energy and for a Compton parameter $Y < 10^{-2}$. This cut-off energy, around 1 GeV for the terrestrial observer, could be directly observable for sufficient short GRBs (i.e $\Delta t_w < \text{a few tens of seconds}$) and for reasonable luminosity (i.e $L_\gamma^{\text{iso}} \simeq 10^{51} \text{ erg}\cdot\text{s}^{-1}$), by the new *Fermi* observatory.
- For $1.4 \lesssim \alpha \lesssim 2$, we cannot observe directly any highest cut-off energy in the electronic synchrotron spectrum, but this energy could be easily deduced from the observation of the instantaneous cut-off energy during the prompt emission stage and, more particularly, from its variations with time, as described in Sec. 3.2.
- For a low level of turbulence ($\eta_t < 10^{-3}$), and whatever the magnetic field index α , there is no γ - γ absorption. However, the highest energy cut-off of the electronic synchrotron spectrum does not correspond to the previous cut-off energy $\epsilon_{c,\text{syn}}^e$, and it only results from the comparison between t_{acc} and t_{dyn} at the very beginning of the internal shock stage (i.e at r_b). Also, it is important to note that this early cut-off energy is not dependent on the magnetic field index. In this case, the electronic population would undergo a pure slow cooling regime, but the adiabatic cooling is too strong and the acceleration process cannot start.
- At last, for a low turbulence level, the UHECR generation could be also compromise, because of inefficiency of the primary acceleration process in the internal shocks (see Eq. (26) with $\kappa_0 \gg 10$) and, consequently, a too weak energy of injection in any secondary acceleration process.

We emphasize that any observability of the electron distribution cut-off or of the UHECR synchrotron emission would stem from a detailed analysis of the spectrum temporal evolution; no single zone modeling of the emissions will provide with this important diagnosis. The diagnosis of magnetic parameters through the spectrum evolution seems already at hand with *Fermi* observations.

Appendix 1: Cut-off energy of the electronic population in the internal shock stage

The Fermi acceleration (first and second order) in the internal and mildly relativistic shocks was first considered by Waxman (1995) with a characteristic acceleration time proportional to Larmor's time of accelerated particles (Bohm scaling). We showed in a previous paper (Gialis & Pelletier 2003) that, in a more realistic situation, Fermi's acceleration time in the internal shocks depends on the mean free path of the particle, namely $\bar{\ell}$, in an irregular magnetic field. Assuming a turbulence spectrum of magnetic perturbations that follows a power law of index β , on both sides of the shock, we have

$$\bar{\ell} = \frac{r_L}{\eta_t} \left(\frac{r_L}{\ell_c} \right)^{1-\beta}, \quad (34)$$

for Larmor's time $r_L < \ell_c$, with $\eta_t \equiv \frac{\langle \delta B^2 \rangle}{\langle B^2 \rangle}$ the turbulence level, and ℓ_c the magnetic correlation length, which is of the order of the layer thickness i.e $\simeq r/\eta$ beyond the radius r_b . Eq. (34) is known in weak turbulence theory and has been extended into the regime of strong turbulence (Casse et al. 2002). Then, the acceleration time t_{acc} is given by

$$t_{\text{acc}} \simeq \frac{2^{1-\beta} |\mu|^{1-\beta} \bar{\ell}}{3\pi^\beta (\beta-1) c}, \quad (35)$$

where μ is the cosine of the pitch angle.

We suppose that layers start to expand by carrying a magnetic field the intensity of which decays like $r^{-\alpha}$ ($1 \leq \alpha < 2$), and is equal to $B_b \simeq 10^5 \text{ G}$ at r_b . According to the equation (35), the acceleration time, in the co-moving frame, for an electron is (c.g.s units)

$$t_{\text{acc}} \simeq C_1(\beta) \left(\frac{\kappa_0}{10} \right) \eta^{1-\beta} (B_b r_b^\alpha)^{\beta-2} \epsilon^{2-\beta} r^{(\beta-1)+\alpha(2-\beta)}, \quad (36)$$

where ϵ is the energy of the electron, e is elementary charge, $\kappa_0 (\equiv \frac{|\mu|^{1-\beta}}{2\pi\eta_t})$, the ratio of the acceleration time over Larmor's time for $r_L = \ell_c$, and the coefficient

$$C_1(\beta) = \frac{20 (2\pi)^{1-\beta} e^{\beta-2}}{3 (\beta-1) c}. \quad (37)$$

The acceleration process is clearly more efficient for a value of α close to 1 i.e for a slow decaying magnetic field.

In the internal shock stage, we obtain the electron maximal energy by comparing the acceleration time with the characteristic synchrotron loss time. This energy, namely ϵ_{syn} and calculated in the co-moving frame, is the synchrotron limitation

$$\epsilon_{\text{syn}} = C_2(\beta) \left(\frac{\kappa_0}{10} \right)^{\frac{1}{\beta-3}} \eta^{\frac{1-\beta}{\beta-3}} (B_b r_b^\alpha)^{\frac{\beta}{\beta-3}} r^{s_1}, \quad (38)$$

where the index s_1 can be written as

$$s_1 = \frac{1 + \beta(\alpha - 1)}{3 - \beta}, \quad (39)$$

and the coefficient $C_2(\beta)$ as

$$C_2(\beta) = \left(\frac{6\pi m_e^2 c^3}{\sigma_T C_1(\beta)} \right)^{\frac{1}{3-\beta}}. \quad (40)$$

For $\alpha = 1$, and a Kolmogorov scaling with $\beta = 5/3$, this limitation can be expressed as

$$\epsilon_{\text{syn}} = 210 \left(\frac{\kappa_0}{10} \right)^{-3/4} \left(\frac{\eta}{100} \right)^{-2} \left(\frac{B_b}{10^5 \text{ G}} \right)^{-5/4} \left(\frac{r_0}{10^7 \text{ cm}} \right)^{-5/4} \left(\frac{r}{10^{11} \text{ cm}} \right)^{3/4} \text{ MeV}. \quad (41)$$

Another limitation comes from adiabatic cooling due to the relativistic expansion of the layer. Comparing the characteristic dynamical time ($\simeq r/c\eta$) with the acceleration time leads to a new limitation for the energy of the electrons. This expansion limitation, namely ϵ_{exp} and calculated in the co-moving frame, is such that

$$\epsilon_{\text{exp}} = (c C_1(\beta))^{\frac{1}{\beta-2}} \left(\frac{\kappa_0}{10} \right)^{\frac{1}{\beta-2}} \eta^{-1} B_b r_b^\alpha r^{s_2}, \quad (42)$$

where the index s_2 is equal to $1 - \alpha$. For $\alpha = 1$, and $\beta = 5/3$, we have

$$\epsilon_{\text{exp}} = 1.2 \times 10^9 \left(\frac{\kappa_0}{10} \right)^{-3} \left(\frac{\eta}{100} \right) \left(\frac{B_b}{10^5 \text{ G}} \right) \left(\frac{r_0}{10^7 \text{ cm}} \right) \text{ MeV}. \quad (43)$$

The transition radius r_c between these two limitations can be easily obtained:

$$r_c = \Lambda(\alpha, \beta) \left(\frac{\kappa_0}{10} \right)^{\frac{1}{(\beta-2)(3\alpha-2)}} \eta^{\frac{2}{2-3\alpha}} (B_b r_b^\alpha)^{\frac{3}{3\alpha-2}}, \quad (44)$$

where the coefficient is such that

$$\Lambda(\alpha, \beta) = \left(\frac{20 (2\pi)^{1-\beta}}{3(\beta-1)} \right)^{\frac{3-\beta}{(\beta-2)(3\alpha-2)}} \left(\frac{9\pi m_e^2 c^4 (\beta-1)}{10 \sigma_T (2\pi)^{1-\beta} e} \right)^{\frac{1}{2-3\alpha}}. \quad (45)$$

For $\alpha = 1$ and $\beta = 5/3$, the distance may be close to r_d ;

$$r_c = 1.0 \times 10^{20} \left(\frac{\kappa_0}{10} \right)^{-3} \left(\frac{\eta}{100} \right)^4 \left(\frac{B_b}{10^5 G} \right)^3 \left(\frac{r_0}{10^7 \text{ cm}} \right)^3 \text{ cm}. \quad (46)$$

Thus, during the expansion, the electron energy distribution undergoes a two stage self-similar evolution, that depends on magnetic parameters.

For an electron in a magnetic field B , the synchrotron emission reaches a maximum power close to the cut-off energy

$$\epsilon_{\max} \simeq \frac{h e B}{4 m_e^3 c^5} \epsilon^2, \quad (47)$$

where ϵ is the energy of the electron.

According to Eq. (38), for $r_b \leq r \leq r_c$, this energy, in the observer frame, can be expressed as

$$\epsilon_{\max}^{\text{syn}} \simeq \frac{h e}{4 m_e^3 c^5} C_2^2(\beta) \left(\frac{\kappa_0}{10} \right)^{\frac{2}{\beta-3}} \eta^{\frac{1+\beta}{3-\beta}} (B_b r_b^\alpha)^{\frac{3(1-\beta)}{3-\beta}} r^{2s_1-\alpha}. \quad (48)$$

And Eq. (42) leads to the evolution for $r \geq r_c$, which is $\propto r^{2-3\alpha}$;

$$\epsilon_{\max}^{\text{syn}} \simeq \frac{h e}{4 m_e^3 c^5} (c C_1(\beta))^{\frac{2}{\beta-2}} \left(\frac{\kappa_0}{10} \right)^{\frac{2}{\beta-2}} \eta^{-1} (B_b r_b^\alpha)^3 r^{2-3\alpha}. \quad (49)$$

The energy ϵ_c at the break radius r_c is given by

$$\epsilon_c \simeq 4.4 \times 10^{-8} (c C_1(\beta))^{\frac{2}{\beta-2}} \left(\frac{20 (2\pi)^{1-\beta}}{3(\beta-1)} \right)^{\frac{\beta-3}{\beta-2}} \left(\frac{9\pi m_e^2 c^4 (\beta-1)}{10 \sigma_T (2\pi)^{1-\beta} e} \right) \left(\frac{\kappa_0}{10} \right)^{\frac{1}{\beta-2}} \eta.$$

For $r \simeq r_b$ and according to Eq. (48), one can write the initial $\epsilon_{\max}^{\text{syn}}$, namely ϵ_{peak}^i , as

$$\epsilon_{\text{peak}}^i \propto \eta^{\frac{\lambda}{3-\beta}} \eta_t^{\frac{2}{3-\beta}} \left(\frac{\Omega c \Delta t_w}{r_0} \right)^{\frac{3}{2} \frac{\beta-1}{3-\beta}} \left(M_{\text{BH}}^{5/2} E_{\text{mag}}^{-3/2} \right)^{\frac{\beta-1}{3-\beta}}, \quad (50)$$

where E_{mag} is the magnetic energy released by the burst, M_{BH} the mass of the inner black hole, and $\lambda = 5 - 3\beta + 6\alpha(\beta - 1)$. Assuming that $E_{\text{mag}} \propto E$ and $M_{\text{BH}} \propto E$, this relation yields to a kind of Amati's law involving β only:

$$\epsilon_{\text{peak}}^i \propto E^{\frac{\beta-1}{3-\beta}}. \quad (51)$$

Appendix 2: Determination of the local electronic synchrotron spectrum

In this Appendix, we propose to determine the electronic distribution and the resulting synchrotron spectrum locally produced, which both depend on the distance from the central engine: we usually distinguish two cooling regimes for the electronic population (Sari et al. (1998), Gupta & Zhang (2007)) separating by the condition $t_{\text{syn}} = t_{\text{dyn}}$ corresponding to a critical Lorentz factor:

$$\gamma_{\text{cr}} \simeq 2.3 \left(\frac{\eta}{100} \right) \left(\frac{B_b}{10^5 \text{ G}} \right)^{-2} \left(\frac{r}{r_b} \right)^{2\alpha-1}. \quad (52)$$

An electron, with a Lorentz factor γ_e , undergoes a fast cooling regime if $\gamma_e > \gamma_{\text{cr}}$ and, a slow cooling regime otherwise. The transition radius, r_t , for which $\gamma_{\text{cr}} = \gamma_{e,\text{min}}$, is

$$r_t \simeq \left[174 \left(\frac{\gamma_{e,\text{min}}}{400} \right) \left(\frac{\eta}{100} \right)^{-1} \left(\frac{B_b}{10^5 \text{ G}} \right)^2 \right]^{\frac{1}{2\alpha-1}} r_b. \quad (53)$$

Obviously, whatever $\alpha \in [1, 2]$, $r_b < r_t < r_c$. Then, because of the outflow evolution during the expansion, we show that accelerated electrons undergo these two cooling regimes (see Fig. 9). Indeed, let be $f(\epsilon, t)$, the electronic distribution, at a time t in the co-moving frame. According to the acceleration process, the continuity equation, for the fast cooling regime, can be simply expressed as

$$\frac{\partial f}{\partial t} + \frac{\partial}{\partial \epsilon} (\dot{\epsilon} f) \propto \epsilon^{-p}, \quad (54)$$

by assuming that $t_{\text{acc}} \ll t_{\text{syn}}$, and only considering synchrotron losses, i.e $\dot{\epsilon} \propto \epsilon^2$. In the stationary case ($\partial/\partial t \equiv 0$), we deduce that $f(\epsilon, t) \propto \epsilon^{-(p+1)}$. In slow cooling regime, the distribution is mainly governed by the acceleration process, i.e $f(\epsilon, t) \propto \epsilon^{-p}$. Thus, during the expansion, and in the co-moving frame, we derive the following results, without taking account of the thermal component for $\epsilon < \epsilon_{\text{min}}^e$:

- When $\gamma_{e,\text{min}} > \gamma_{\text{cr}}$, which is always the case at the very beginning of the internal shock phase,

$$\frac{dn_e}{d\epsilon} \propto \begin{cases} \epsilon^{-2} & \text{for } \epsilon_{\text{cr}} < \epsilon < \epsilon_{\text{min}}^e \\ \epsilon^{-(p+1)} & \text{for } \epsilon_{\text{min}}^e < \epsilon < \epsilon_{\text{max}}^e \end{cases}, \quad (55)$$

where $\epsilon_{\text{min}}^e = \gamma_{e,\text{min}} m_e c^2$ and $\epsilon_{\text{cr}} = \gamma_{\text{cr}} m_e c^2$. This is a “pure” fast cooling regime for all the accelerated electrons. The corresponding synchrotron photon distribution, in the co-moving frame, is

$$\frac{dn_\gamma}{d\epsilon} \propto \begin{cases} \epsilon^{-2/3} & \text{for } \epsilon < \epsilon_{\text{syn}}^{\text{cr}} \\ \epsilon^{-3/2} & \text{for } \epsilon_{\text{syn}}^{\text{cr}} < \epsilon < \epsilon_{\text{syn}}^{\text{low}} \\ \epsilon^{-(p+2)/2} & \text{for } \epsilon_{\text{syn}}^{\text{low}} < \epsilon < \epsilon_{\text{syn}}^{\text{max}} \end{cases}, \quad (56)$$

where we define $\epsilon_{\text{syn}}^{\text{cr}} \simeq 3h e B \gamma_{\text{cr}}^2 / (4\pi m_e c)$ for $\gamma_{\text{cr}} > 1$. More precisely, the scaling is the following one

$$\epsilon_{\text{syn}}^{\text{cr}} \simeq 9.2 \times 10^{-6} \left(\frac{\eta}{100} \right)^2 \left(\frac{B_b}{10^5 \text{ G}} \right)^{-3} \left(\frac{r}{r_b} \right)^{3\alpha-2} \text{ keV}. \quad (57)$$

- When $\gamma_{e,\text{min}} < \gamma_{\text{cr}} < \gamma_{e,\text{max}}$, which is always the case between r_t and r_c ,

$$\frac{dn_e}{d\epsilon} \propto \begin{cases} \epsilon^{-p} & \text{for } \epsilon_{\text{min}}^e < \epsilon < \epsilon_{\text{cr}} \\ \epsilon^{-(p+1)} & \text{for } \epsilon_{\text{cr}} < \epsilon < \epsilon_{\text{max}}^e \end{cases}. \quad (58)$$

This situation mixes the two cooling regimes for the accelerated electron population and, the synchrotron photon distribution, in the co-moving frame, is

$$\frac{dn_\gamma}{d\epsilon} \propto \begin{cases} \epsilon^{-2/3} & \text{for } \epsilon < \epsilon_{\text{syn}}^{\text{low}} \\ \epsilon^{-(p+1)/2} & \text{for } \epsilon_{\text{syn}}^{\text{low}} < \epsilon < \epsilon_{\text{syn}}^{\text{cr}} \\ \epsilon^{-(p+2)/2} & \text{for } \epsilon_{\text{syn}}^{\text{cr}} < \epsilon < \epsilon_{\text{syn}}^{\text{max}} \end{cases}. \quad (59)$$

- When $\gamma_{\text{cr}} > \gamma_{e,\text{max}}$, which is always the case beyond the cooling radius r_c ,

$$\frac{dn_e}{d\epsilon} \propto \epsilon^{-p} \text{ for } \epsilon_{\text{min}}^e < \epsilon < \epsilon_{\text{max}}^e. \quad (60)$$

This is a “pure” slow cooling regime for the accelerated electrons. Here, the synchrotron photon distribution is simply

$$\frac{dn_\gamma}{d\epsilon} \propto \begin{cases} \epsilon^{-2/3} & \text{for } \epsilon < \epsilon_{\text{syn}}^{\text{low}} \\ \epsilon^{-(p+1)/2} & \text{for } \epsilon_{\text{syn}}^{\text{low}} < \epsilon < \epsilon_{\text{syn}}^{\text{max}} \end{cases}. \quad (61)$$

The resulting synchrotron photon distribution can be numerically calculated by the integration of the previous local distributions, all along the outflow. The obtained result is really different from the previous works (see e.g. Gupta & Zhang (2007)) because it takes into account both the important stratification of the outflow and a precise cut-off energy, in the local electronic synchrotron spectrum, resulting from a detailed analysis of the acceleration process. This point will be fully detailed in a forthcoming paper. However, in this paper, we have just assumed that the resulting photon distribution is given by a phenomenological Band’s function (Band et al. (1993)).

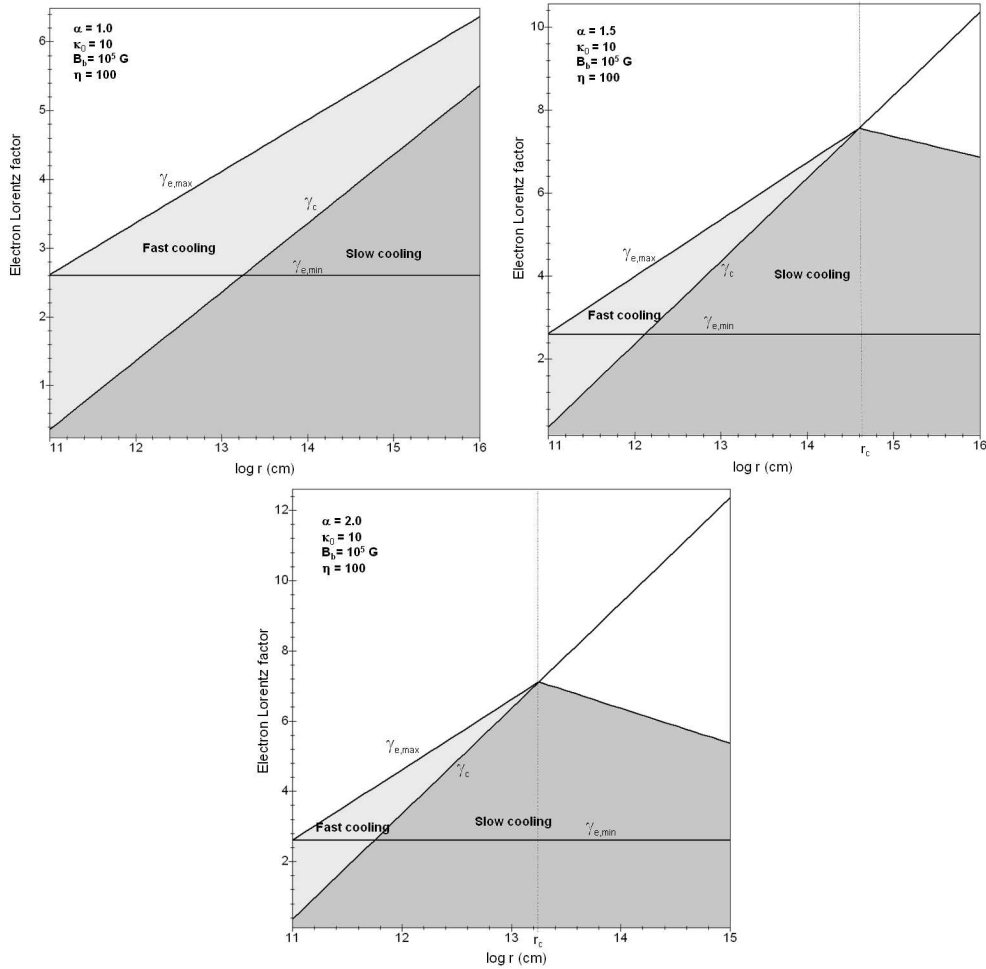


Fig. 9. Variation of the upper ($\gamma_{e,\max}$) and lower ($\gamma_{e,\min}$) bounds for the electronic Lorentz factor distribution, for three different magnetic field index α , and beyond r_b . The critical Lorentz factor, γ_{cr} , separates the accelerated electron distribution in two different regimes: the fast cooling regime and the slow one.

References

- Asano, K. & Inoue, S. 2007, ApJ, 671, 645
 Band, D., Matteson, J., Ford, L., et al. 1993, ApJ, 413, 281
 Bell, A. R. 1978, MNRAS, 182, 147
 Blandford, R. D. & Ostriker, J. P. 1978, ApJL, 221, L29
 Casse, F., Lemoine, M., & Pelletier, G. 2002, Phys. Rev. D, 65, 023002
 Drury, L. O. 1983, Reports of Progress in Physics, 46, 973
 Gialis, D. & Pelletier, G. 2003, Astrop. Phys., 20, 323
 Gialis, D. & Pelletier, G. 2004, A & A, 425, 395
 Gialis, D. & Pelletier, G. 2005, ApJ, 627, 868
 Gould, R. J. & Schröder, G. P. 1967, Phys. Rev., 155, 1404
 Granot, J., Cohen-Tanugi, J., & do Couto e Silva, E. 2008, ApJ, 677, 92
 Gupta, N. & Zhang, B. 2007, MNRAS, 380, 78
 Lacombe, C. 1977, A&A, 54, 1
 Lemoine, M., Pelletier, G., & Revenu, B. 2006, ApJL, 645, L129
 Pe'er, A. & Waxman, E. 2004, ApJ, 613, 448
 Piran, T. 2005, Reviews of Modern Physics, 76, 1143
 Preece, R. D., Briggs, M. S., Malozzi, R. S., et al. 2000, ApJS, 126, 19
 Rees, M. J. & Mészáros, P. 1994, ApJL, 430, L93
 Sari, R., Piran, T., & Narayan, R. 1998, ApJL, 497, L17+
 Waxman, E. 1995, Phys. Rev. Lett., 75, 386